Revista ION e-ISSN: 2145-8480 ISSN-L: 0120-100X DOI: https://doi.org/10.18273/revion.v38n1-2025006

Theoretical Vibrational Study of Metformin: A DFT-Based Analysis of Simulated Raman and SERS Spectra

Ciro E. Rozo Correa[1]; Juan José Blanco Prada[2]; John Jairo Castillo León[3,4a]

[1]Grupo de Investigaciones Ambientales para el Desarrollo Sostenible, Universidad Santo Tomás, Bucaramanga, Colombia.
[2]Grupo de Investigación en Bioquímica y Microbiología GIBIM, [3]Laboratorio de Espectroscopia Atómica y Molecular y Molecular (LEAM), Universidad Industrial de Santander, Bucaramanga, Colombia.
[4]Center for Intelligent Drug Delivery and Sensing Using Microcontainers and Nanomechanics (IDUN), Technical University of Denmark, Denmark.

[a]jcasleon@uis.edu.co; jjcl@dtu.dk

Fecha recepción: 15 de mayo 2025
Fecha aceptación: 04 de septiembre de de 2025

Graphical Abstract

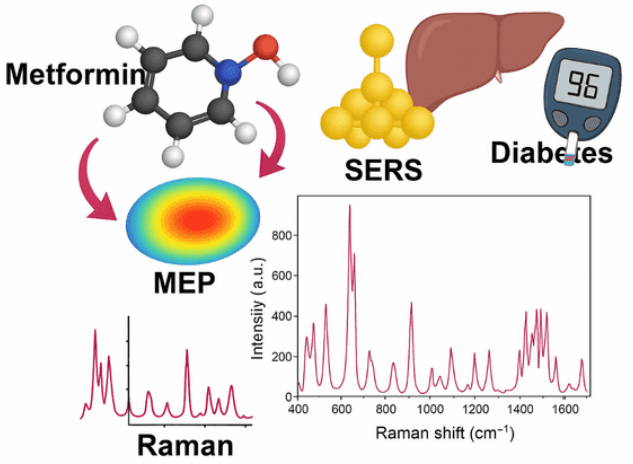

Highlights

1. DFT simulation identifies vibrations and adsorption sites of metformin.
2. Raman and SERS reveal charge transfer with the gold cluster.
3. Theoretical and experimental data closely match, validating the model.

Abstract

Metformin (MET), a widely used antidiabetic drug, has attracted significant attention due to its potential applications beyond diabetes treatment. Understanding its molecular vibrations is crucial for spectroscopic characterization and interaction studies. This study presents a computational investigation of MET using Density Functional Theory (DFT) to analyze its vibrational properties, Raman spectra, and Surface-Enhanced Raman Scattering (SERS) behavior. Geometry optimization at the B3LYP/6-31G(d) level identified the most stable conformer, and a molecular electrostatic potential map highlighted key electron-rich sites for adsorption. Raman spectra were simulated using the B3LYP/6-31G(d) level, providing theoretical insights into MET's vibrational modes. The interaction of MET with a gold cluster, modeled using the LanL2DZ basis set, revealed charge transfer effects influencing SERS enhancement. Theoretical Raman and SERS spectra, scaled for accuracy, closely matched experimental results, confirming MET's characteristic vibrational signatures. This combined approach offers valuable insights into MET's adsorption mechanisms and vibrational response, enhancing its potential application in electrochemical and spectroscopic sensing technologies.

Keywords: *Metformin; Diabetes; DFT Calculations; Raman Spectroscopy; Surface-Enhanced Raman Spectroscopy*.

Cita: Rozo Correa CE, Blanco Prada JJ, Castillo León JJ. Theoretical Vibrational Study of Metformin: A DFT-Based Analysis of Simulated Raman and SERS Spectra. rev. ion. 2025;38(1):101-115. https://doi.org/10.18273/revion.v38n1-2025006

Estudio vibracional teórico de la metformina: un análisis basado en DFT de espectros Raman y SERS simulados

Resumen
La metformina (MET), un fármaco antidiabético de uso ampliamente extendido, ha despertado un notable interés debido a sus posibles aplicaciones más allá del tratamiento de la diabetes. Comprender sus vibraciones moleculares es crucial para la caracterización espectroscópica y el estudio de sus interacciones. Este estudio presenta una investigación computacional de MET utilizando la Teoría del Funcional de la Densidad (DFT) para analizar sus propiedades vibracionales, espectros Raman y comportamiento en espectroscopía Raman mejorada por superficie (SERS). La optimización de geometría a nivel B3LYP/6-31G(d) permitió identificar el confórmero más estable, y un mapa de potencial electrostático molecular destacó los sitios clave ricos en electrones para la adsorción. Los espectros Raman fueron simulados utilizando el mismo nivel teórico, proporcionando información sobre los modos vibracionales de MET. La interacción de MET con un clúster de oro, modelada usando la base LanL2DZ, reveló efectos de transferencia de carga que influyen en la mejora SERS. Los espectros Raman y SERS teóricos, ajustados para mayor precisión, coincidieron estrechamente con los resultados experimentales, confirmando las firmas vibracionales características de MET. Este enfoque combinado ofrece información valiosa sobre los mecanismos de adsorción y la respuesta vibracional de MET, mejorando su potencial aplicación en tecnologías de detección electroquímica y espectroscópica.

Palabras clave: *Metformina; Diabetes; Cálculos DFT; Espectroscopía Raman; Espectroscopía Raman mejorada por superficie.*

Estudo vibracional teórico da metformina: uma análise baseada em DFT de espectros Raman e SERS simulados

Resumo
A metformina (MET), um fármaco amplamente utilizado no tratamento do diabetes, tem despertado interesse significativo devido às suas potenciais aplicações além do controle glicêmico. A compreensão de suas vibrações moleculares é essencial para a caracterização espectroscópica e estudos de interação. Este estudo apresenta uma investigação computacional da MET utilizando a Teoria do Funcional da Densidade (DFT) para analisar suas propriedades vibracionais, espectros Raman e comportamento em Espalhamento Raman Intensificado por Superfície (SERS). A otimização geométrica no nível B3LYP/6-31G(d) permitiu identificar o confórmero mais estável, e o mapa de potencial eletrostático molecular evidenciou regiões eletronicamente ricas propensas à adsorção. Os espectros Raman foram simulados no mesmo nível teórico, fornecendo informações sobre os modos vibracionais da MET. A interação com um aglomerado de ouro, modelado com o conjunto de base LanL2DZ, revelou efeitos de transferência de carga que influenciam a intensificação SERS. Os espectros Raman e SERS teóricos, ajustados para maior precisão, mostraram boa concordância com os resultados experimentais, confirmando as assinaturas vibracionais características da MET. Esta abordagem combinada oferece insights relevantes sobre os mecanismos de adsorção e resposta vibracional da MET, ampliando seu potencial em tecnologias de detecção eletroquímica e espectroscópica.

Palavras-chave*: Metformina; Diabetes; Cálculos DFT; Espectroscopia Raman; Espectroscopia Raman Intensificada por Superfície.*

Introduction

Metformin (MET), a widely used medication in the treatment of type 2 diabetes mellitus, has become one of the most important drugs in modern medicine due to its effectiveness in managing blood glucose levels [1-3]. As a member of the biguanide class, metformin has been extensively studied for its pharmacological properties, mechanisms of action, and clinical applications [4,5]. It is known to improve insulin sensitivity, reduce hepatic glucose production, and enhance peripheral glucose uptake, making it a cornerstone of diabetes management [6]. Despite its proven efficacy, understanding the molecular interactions and structural properties of metformin remains an ongoing area of research, particularly in the context of its spectroscopic characterization.

The vibrational properties of MET are crucial for its molecular identification and the analysis of its interactions with biological systems. Vibrational spectroscopy techniques, such as Raman and Surface-Enhanced Raman Spectroscopy (SERS), are powerful tools for probing the molecular structure and dynamics of organic compounds [7-13]. These techniques provide valuable information about the internal vibrations of molecules, which can be linked to functional groups and molecular symmetry. However, experimental studies often face limitations in providing detailed insights, especially when examining complex molecular systems like MET. Therefore, computational studies using methods such as DFT offer a complementary approach to explore the vibrational properties of molecules at a molecular level [14]. To aid in the understanding of MET's molecular structure, a 3D representation of the molecule is provided (Figure 1). This model illustrates the spatial arrangement of atoms within the MET molecule, highlighting key functional groups such as the guanidine and amine moieties. DFT is a quantum mechanical method used to investigate the electronic structure of atoms, molecules, and solids. Unlike other quantum mechanical methods such as Hartree-Fock theory, DFT focuses on the electron density rather than the many-electron wavefunction, making it computationally more efficient for larger systems [14-17]. Common functionals used in DFT calculations include B3LYP, PBE0, and others, each with varying degrees of accuracy depending on the system under study [17-19]. For this study, the B3LYP functional was selected due to its balance between computational efficiency and accuracy for organic molecules. Additionally, the choice of basis set is important in DFT calculations, as it defines the functions used to describe the orbitals of the atoms in the molecule. For this study, a commonly used basis set for organic molecules is 6-31G*, which provides a good balance of accuracy and computational cost [20]. The molecular geometry of MET was optimized using DFT, ensuring that the calculated vibrational modes correspond to the molecule's true equilibrium structure.

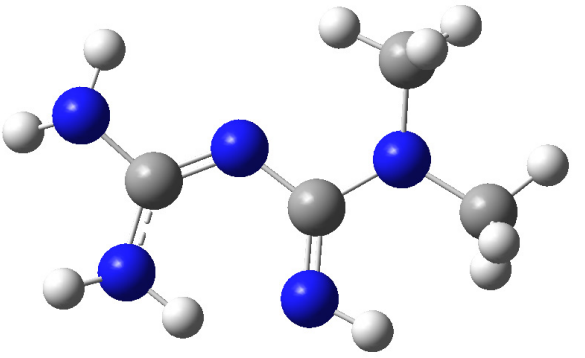

Figure 1. 3D molecular structure of MET. The 3D representation highlights the key atomic arrangement and bonding interactions relevant to vibrational analysis. Color scheme: carbon (gray), nitrogen (blue), hydrogen (white).

Several theoretical studies have explored the geometry and vibrational properties of MET, including its interaction with counterions or in solid-state formulations [14]. However, there is a notable gap in the literature regarding the modeling of metformin's interaction with metallic surfaces relevant to SERS applications. To the best of our knowledge, no prior study has combined DFT-based Raman and SERS simulations with MEP mapping and adsorption onto gold clusters.

Raman spectroscopy is a powerful technique used to probe the vibrational modes of molecules [21,22]. It is based on the inelastic scattering of light, where photons interact with the vibrational modes of a molecule and loss or gain energy, resulting in a shift in the frequency of the scattered light. The Raman spectrum provides information about the bond strengths, functional groups, and molecular symmetry, making it an invaluable tool for studying molecular structures. In the case of MET, Raman spectroscopy can be used to identify the characteristic vibrational modes associated with its molecular structure, such as the C-N stretching

and N-H bending vibrations. The Raman spectrum of MET can provide insights into its functional groups and the overall symmetry of the molecule, allowing for a more detailed understanding of its molecular properties. The theoretical Raman spectra obtained through DFT calculations can be compared with experimental spectra to identify the vibrational modes and assign them to specific molecular vibrations [23,24]. The calculated Raman spectra can also be used to study the effect of different environments on metformin's vibrational properties, such as the presence of solvents or the interaction with surfaces. These computational studies can guide experimentalists in interpreting Raman spectra and designing more efficient experiments for analyzing MET and similar molecules.

SERS is an advanced variation of Raman spectroscopy that significantly enhances the Raman signal through the interaction of molecules with metallic surfaces, typically made of silver, gold, or copper [21,22,25]. The enhancement arises from two main effects: the electromagnetic effect and the chemical effect. The electromagnetic effect occurs due to the localized surface plasmon resonance (LSPR) of metallic nanoparticles, which can concentrate light near the surface and enhance the Raman scattering signal. The chemical effect arises from the interactions between the molecule and the metal surface, which can alter the vibrational frequencies and intensities. SERS has become a powerful tool for detecting trace amounts of molecules, especially in applications such as biosensing, environmental monitoring, and chemical analysis [26,27]. The enhancement of the Raman signal allows for the detection of molecules at very low concentrations, making SERS particularly valuable for studying compounds like MET in complex matrices, where traditional Raman spectroscopy may not be sensitive enough [27-30]. This enhancement is due to localized surface plasmon resonance (LSPR) and chemical interactions between the molecule and the metal surface, making SERS a highly sensitive technique for molecular detection [31].

In this study, DFT calculations are employed to simulate Raman vibrational spectra and the interaction between MET and a 10-gold atom cluster, to predict how these interactions might affect the SERS spectra. By modeling the geometry of the metal surface and the adsorption of MET, it is possible to simulate the enhanced Raman signals that would be observed experimentally. This theoretical approach provides a deeper understanding of how the molecular vibrations of MET are influenced by the surface and how SERS can be used to enhance its detection. To date, however, there are few computational studies that focus on the SERS and Raman simulations, as well as the adsorption behavior of MET on gold substrates. Although some theoretical studies on metformin have been reported [14], the literature remains scarce with respect to combined Raman and SERS simulations including adsorption onto metallic surfaces. Therefore, a detailed comparative analysis was not feasible. However, the cited works have been used to contextualize and contrast the scope and methodology of the present study. Finally, this work aims to bridge this gap by providing a detailed computational framework that will help to predict and interpret the experimental SERS signals of MET.

Methodology

Geometry Optimization and Energy Structure

To investigate the vibrational properties of MET and its SERS characteristics, a comprehensive computational study was performed using DFT. All calculations were carried out using the Gaussian software package [32], employing functionals and basis sets tailored for both isolated molecular structures and metal-molecule interactions. The first stage of the computational workflow involved the geometry optimization of MET in the gas phase, aiming to obtain its most stable conformer. The optimization was performed using the B3LYP functional (Becke's three-parameter hybrid functional with Lee-Yang-Parr correlation) and the 6-31G(d) basis set, which has been widely employed in molecular vibrational studies due to its balanced trade-off between computational cost and accuracy [18,19]. The absence of imaginary vibrational frequencies in the optimized structure confirmed that the resulting geometry corresponded to a global or local minimum on the potential energy surface (PES).

To simulate the SERS environment, an additional system was constructed where MET was placed in close interaction a 10-gold atom cluster, serving as a minimalistic representation of the metal surface. Since gold is a heavy element with significant relativistic effects, its electronic structure was treated using the LanL2DZ (Los Alamos National Laboratory double-zeta) basis set, which includes effective core potentials (ECPs) to model relativistic

contributions [23]. The MET-Au system was optimized at the B3LYP/LanL2DZ level of theory, ensuring that both molecular and metal interactions were accurately described.

The molecular potential energy map of MET was generated using a combination of Gaussian and Visual Molecular Dynamics (VMD) [33,34]. First, the molecular structure of MTF was optimized at the DFT/B3LYP level using a 6-31G(d) basis set in Gaussian. The optimized geometry was then used to compute the electrostatic potential (ESP) using the same functional and basis set. The ESP data were extracted and visualized in VMD, where a color-coded potential energy map was projected onto the molecular surface. The visualization enabled the identification of regions with higher or lower electrostatic potential, which is relevant for understanding molecular interactions, including hydrogen bonding and adsorption on electrode surfaces [35].

Raman and SERS Vibrational Frequency Calculations

After geometry optimization, vibrational frequency calculations were performed at the same levels of theory used for optimization. Raman and SERS spectra were simulated to analyze the vibrational modes of MET in both free and surface-bound states. The harmonic vibrational frequencies were scaled using appropriate correction factors: 0.9614 for Raman and 0.977 for SERS spectra [36]. These scaling factors account for systematic overestimations inherent in DFT calculations due to the harmonic approximation. The Raman activities were obtained from the computed polarizability derivatives, and the corresponding intensities were derived using standard expressions that consider the excitation wavelength-dependent scattering cross-section [19]. For the SERS analysis, the interaction between MET and the gold cluster was evaluated by analyzing vibrational mode shifts and intensity enhancements due to charge transfer and chemical interactions. The spectral features of both Raman and SERS were compared to assess the impact of molecular adsorption on vibrational properties.

Computational Considerations

All calculations were performed in the gas phase to isolate intrinsic molecular vibrational properties. The absence of imaginary frequencies confirmed that the optimized structures correspond to true minima on the potential energy surface. The choice of basis sets 6-31G(d) for MET and LanL2DZ for MET-Au was based on their ability to balance computational cost and accuracy, particularly for molecular interactions with metal atoms [23] for which therapeutic drug monitoring (TDM. Theoretical Raman and SERS spectra were visualized using GaussView software, and normal mode assignments were carried out by comparing computed vibrational modes with literature data. Theoretical results were validated against available experimental spectra to assess the reliability of the computational approach in predicting spectral features.

Results and Discussion

Optimized Geometry and Energy Characteristic of Metformin

Figure 2 presents the optimized molecular structure and conformational analysis of MET. The top panel displays the atomic numbering and molecular geometry obtained from quantum mechanical calculations, which provide critical insights into bond lengths, angles, and electronic distributions. The bottom panel illustrates the different conformers of MET, emphasizing its flexibility and potential variations in dihedral angles due to rotational freedom around single bonds. Computational calculations revealed that conformer a is the most stable, with an energy of -7,390,111.711 kJ/mol, attributed to its near-planar structure and strong intramolecular hydrogen bonding. Conformer b, with a slight deviation from planarity due to steric hindrance, has an energy of -7,303,333.634 kJ/mol. Conformer c, which exhibits the greatest deviation from planarity due to repulsion between adjacent functional groups, has the highest energy at -73,033,145.824 kJ/mol, indicating reduced stability. These energetic differences highlight the importance of hydrogen bonding and steric effects in determining the preferred molecular conformation of MET.

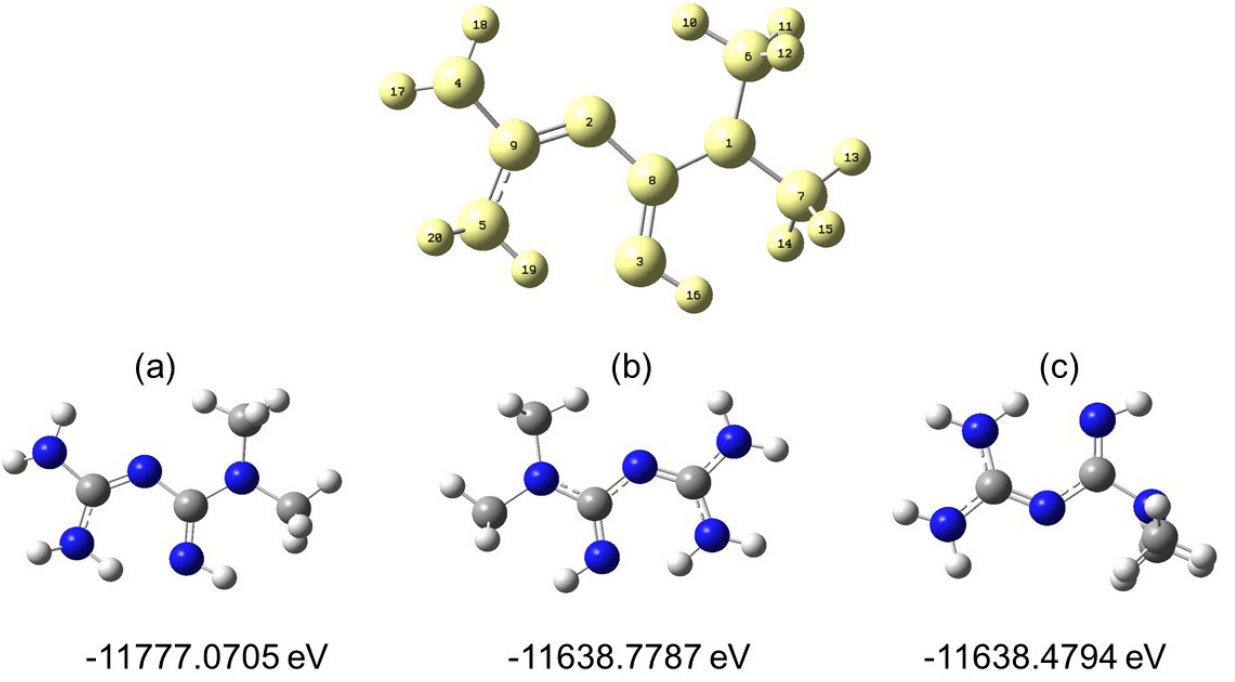

Figure 2. Optimized molecular and conformers of MET obtained by DFT calculations.

The optimized geometry reveals that metformin adopts a nearly planar backbone, with its central guanidine (-NH-C(=NH)-NH_2) and amidine (-N=C-NH_2) groups forming a conjugated electronic system. This delocalization enhances the stability of the molecule and contributes to its characteristic hydrogen bonding interactions. The bond length analysis (as presented in Table 1) indicates that most computed values closely match experimental and previously reported theoretical data, with slight variations due to environmental factors such as solvent effects or crystalline packing forces. The bottom panel highlights the three major conformers of metformin, which differ in the orientation of nitrogen-containing functional groups. These conformers arise from the rotational freedom around the C-N and N-C-N bonds, leading to changes in dihedral angles. The relative stability of each conformer depends on intramolecular hydrogen bonding and steric effects. Notably, conformer a exhibits a near-planar structure with strong intramolecular hydrogen bonding, while conformers b and c display deviations from planarity due to steric hindrance or repulsion between adjacent functional groups. The results are consistent with the optimization of the MET structure in its interaction with ferulic acid, as reported by Makarios *et al.* [14].

The bond lengths obtained for MET were compared to previously reported values from Makarios *et al*. [14]. The N1-C6 (1.455 Å), C8-N3 (1.304 Å), C9-N5 (1.359 Å), and C9-N4 (1.388 Å) bonds exhibit slight variations from the literature, particularly in the case of C8-N3, which is shorter than the reported 1.401 Å. This difference may be attributed to the computational method used or the presence of different molecular environments in experimental and theoretical models. The N4-H18 (1.012 Å) and N5-H20 (1.011 Å) bonds are highly consistent with reported values, with deviations within 0.005 Å, confirming the stability of the protonated amine groups. Interestingly, the C9-N4 (1.388 Å) bond exhibits a deviation from the reported 1.275 Å, suggesting a possible influence of resonance stabilization or hydrogen bonding effects in our model. This discrepancy might arise due to solvation effects or computational settings in the theoretical approach used.

Table 1. Bond distances and dihedral angles of MET.

Bond	Distance (Å)	Makarios *et al.* (Å)[14]	Dihedral Angle (°)
N1-C8	1.392	-	C6-N1-C8 122°
N1-C2	1.456	-	C1-N8=N3 123°
N1-C6	1.455	1.451	N6-C1-N7 116°
C6-H11	1.097	-	C8-N3-H16 113°
C8-N3	1.304	1.401	N4-C9-N2 117°
N3-H16	1.016	-	C9-N2-C8 121°
C8-N2	1.387	-	C6-N1-C8 122°
N2-C9	1.306	-	
C9-N5	1.359	1.400	
C9-N4	1.388	1.275	
N4-H18	1.012	1.017	
N5-H20	1.011	1.011	
N1-C8	1.392	-	
N1-C2	1.456	-	

The dihedral angles calculated for MET provide insights into the molecular conformation. The C6-N1-C8 (122°) and C1-N8=N3 (123°) angles suggest a near-planar arrangement, consistent with an extended conjugation along the molecular backbone. Similar angles were reported by Alzawat *et al*. [37] in their study on the spectral and structural characterization of MET with different counter anions, confirming the structural consistency through DFT calculations. The N6-C1-N7 (116°) angle deviates slightly from planarity, which could indicate steric interactions influencing the flexibility of the molecular structure. Similarly, the C8-N3-H16 (113°) dihedral angle suggests a degree of rotational freedom, particularly in the terminal amine groups. Additionally, the C9-N2-C8 (121°) and N4-C9-N2 (117°) angles reflect conformational adjustments that may result from intramolecular hydrogen bonding or electronic delocalization effects. These results indicate that MET maintains a semi-planar conformation, with deviations arising due to steric and electronic factors. The comparison with Makarios *et al.* [14] *sugguest* that while general trends in bond lengths are preserved, specific variations in C8-N3 and C9-N4 highlight the importance of computational and experimental conditions in determining molecular parameters.

Molecular Electrostatic Potential of Metformin

The molecular electrostatic potential map (MEP) is obtained in this study to provide a detailed understanding of the charge distribution within the MET molecule, which directly influences its vibrational properties and interaction with metal surfaces in SERS experiments [19]. By mapping the electrostatic potential, it is possible to identify regions of electron density that play a crucial role in molecular adsorption and charge transfer processes, which are essential for enhancing Raman signals. Additionally, this analysis aids in correlating theoretical vibrational modes with experimental spectra by offering insights into the electronic environment that governs molecular

polarizability and Raman activity [7,8,11]. Thus, the electric potential map serves as a fundamental tool for interpreting the DFT-based Raman and SERS spectra of MET. As is shown in Figure 3, the MEP map of MET provides a visual representation of the charge distribution within the molecule, highlighting regions of varying electrostatic potential. This is particularly important for understanding the molecule's behavior in intermolecular interactions, such as hydrogen bonding, metal coordination, and charge transfer processes. In our study, blue regions (high electron density, negative potential) correspond to areas where metformin can act as an electron donor. These regions are likely concentrated around the nitrogen atoms of the amine and guanidine functional groups, which have lone pairs of electrons that can participate in hydrogen bonding and metal coordination. On the other side, red zones (low electron density, positive potential) indicate areas where MET can act as an electron acceptor. These are typically associated with hydrogen atoms attached to nitrogen, which are prone to forming hydrogen bonds with electronegative atoms in biological or catalytic systems [36].

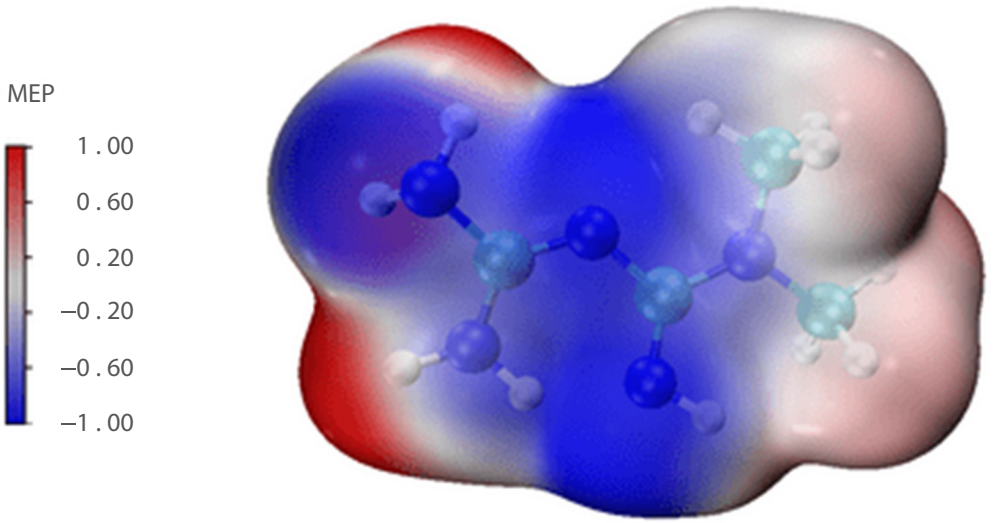

Figure 3. Molecular electrostatic potential map of metformin.

In SERS applications, metformin's interaction with metallic surfaces (e.g., gold or silver nanoparticles) is largely influenced by its electrostatic potential. The electron-rich sites (red) favor adsorption through metal-ligand interactions, particularly via the guanidine and amine functional groups. This influences the enhancement of vibrational modes observed in the Raman spectra. The charge distribution affects the molecular orientation on the surface, which can modulate the enhancement factors of different vibrational bands in the SERS spectrum.

DFT Raman simulation studies

Prior literature has explored the vibrational characteristics and structural properties of MET using both experimental and computational approaches. Yan *et al.* [37] investigated the solid-state conformation of metformin and its hydrogen bonding network by X-ray diffraction and IR spectroscopy, while Cai *et al.* [38] and Ghasemi *et al.* [39] provided DFT-based insights into its vibrational modes in the gas phase. Additionally, Saeed *et al.* [40] reported vibrational features of related guanidine derivatives, which are chemically relevant to the functional groups in MET. However, these studies did not incorporate SERS simulations or metal-surface interactions. In contrast, the present work provides a more integrated perspective by combining DFT simulations of Raman and SERS spectra with MEP analysis and modeling of adsorption on gold clusters, thus offering novel insights into MET's vibrational behavior in plasmonic environments. To improve the accuracy of the computed frequencies, a scaling factor of 0.97 was applied to correct for anharmonic effects and basis set limitations [41]. The simulated Raman intensities reflect the polarizability changes associated with each vibrational mode, providing a direct correlation with experimentally observed

Raman bands. It is important to acknowledge that all vibrational simulations presented in this study were conducted in the gas phase. While this approach is commonly used to extract the intrinsic vibrational characteristics of molecules, it does not consider the influence of aqueous or biological environments, which are relevant for positively charged and hydrophilic drugs like MET. In such media, solvation effects can lead to shifts in vibrational frequencies and changes in intensity, due to hydrogen bonding and dielectric screening. However, incorporating solvation models especially in combination with metallic clusters for SERS simulations significantly increases computational cost. Therefore, the gas phase approximation was chosen to maintain a feasible computational framework while capturing the essential features of MET's vibrational behavior.

The vibrational profile of MET is primarily influenced by its guanidine (-NH-C(=NH)-NH_2) and amidine (-N=C-NH_2) functional groups, which contribute to strong Raman-active modes due to their high polarizability. Additionally, the presence of hydrogen bonding significantly affects the vibrational behavior of the molecule, particularly in the low-wave number region. Table 2 present the detailed band assignments for the computed Raman spectrum, correlating theoretical predictions with experimental data to elucidate the vibrational characteristics of MET.

Table 2. Assignment of calculated Raman vibrational modes of metformin compared with experimental data [42].

Raman Calculated	Raman Measured	SERS Calculated	Proposed Assignment
430	435	426	N4-H18 (rocking)
451	-	-	Skv
466	-	479	Skv
491	-	504	N5-H20 (rocking)
546	-	-	Skv
625	625	-	N5-H19 (rocking)
639	641	662	C17-N4-C18 (rocking)
715	712	720	N3-H16 (rocking)
735	743	-	H14-C7-H15 (scissoring)
824	813	814	C7-H13, C5-H12 (rocking)
836	-	-	N2-C8=N3 (scissoring); N3-H15 (rocking)
919	929	906	C9=N2-C8 (scissoring)
1009	-	1009	H10-C5-H12, H13-C7-H15 (scissoring)
1058	1055	-	H10-C5-H12, H13-C7-H15, N3-H16 (rocking)
1080	1090	1072	H10-C5-H12, H13-C7-H15, N3-H16, H17-N4-H18 (rocking)
1106	1117	1104	H10-C5-H12, H13-C7-H15 (rocking)
1111	-	1119	N4-H18, N5-H19 (rocking)
1144	1154	1186	H10-C5-H12, H13-C7-H15 (rocking)
1208	-	1196	N4-H18, N5-H19, N3-H16 (rocking)
1251	-	1257	H17-N4-H18, H20-N5-H19 (rocking)
1284	1295	1273	H10-C5-H12, H13-C7-H15 (rocking)

The calculated Raman vibrational frequencies of MET were compared with experimental data reported by Baymarov *et al*. [42]. The results, presented in Table 2, demonstrate a strong correlation between theoretical and experimental values, with minor discrepancies that can be attributed to anharmonic effects, environmental influences, and basis set limitations in DFT calculations. Figure 4 shows the DFT-calculated Raman spectrum of MET and complements the information presented in Table 2 by providing a visual representation of the spectrum, allowing for a direct comparison with the experimental values and facilitating the analysis of vibrational mode assignments.

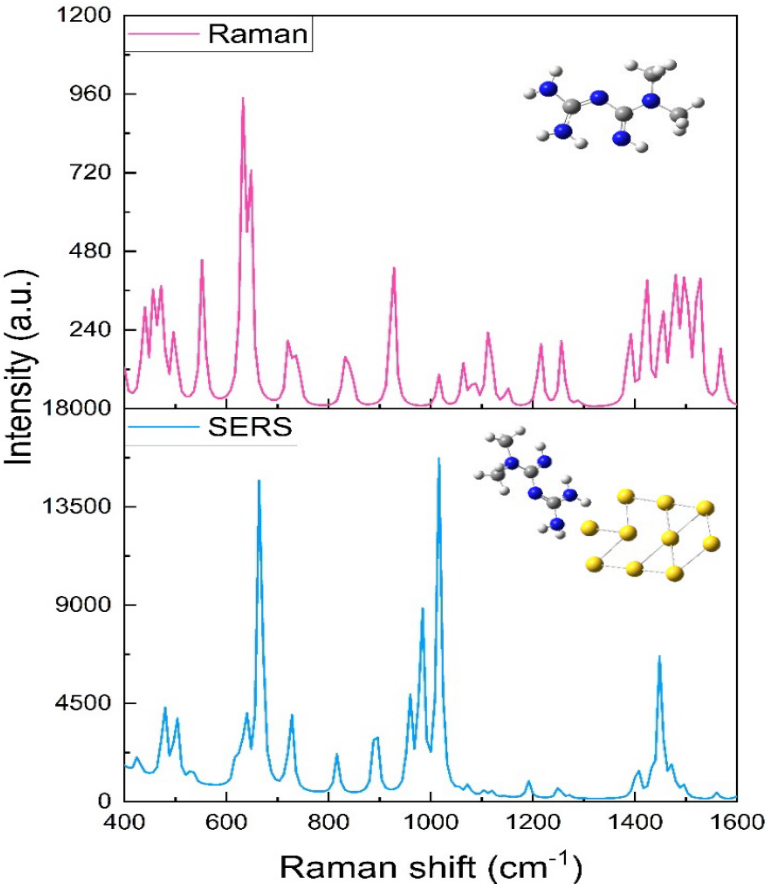

Figure 4. DFT-simulated Raman (-) and SERS (-) spectrum of metformin vibrational modes.

The scissoring motion of H17-N4-H18, calculated at 1668 cm^{-1}, appears experimentally at 1660 cm^{-1}, highlighting the reliability of the DFT-based approach in capturing intramolecular interactions.

• Low-Frequency Region (400 – 700 cm^{-1}):
The N-H rocking modes are prominent in this region, with calculated values at 430 cm^{-1} (N4-H18) and 491 cm^{-1} (N5-H20), showing excellent agreement with the experimental peak at 435 cm^{-1}. The calculated peak at 625 cm^{-1}, assigned to N5-H19 rocking, is observed experimentally at 625 cm^{-1}, indicating a strong correlation between theory and experiment. The C-N rocking mode at 639 cm^{-1} closely matches the experimental value of 641 cm^{-1}, further validating the computational model.

• Mid-Frequency Region (700 – 1300 cm^{-1}):
Several rocking and scissoring modes of C-H and N-H bonds appear in this range, demonstrating consistency between the computational and experimental data. The N3-H16 rocking mode calculated at 715 cm^{-1} closely aligns with the experimental peak at 712 cm^{-1}. The scissoring vibrations of H10-C5-H12 and H13-C7-H15 exhibit slight deviations, with calculated values at 1009 and 1058 cm^{-1}, compared to experimental

values at 1055 cm^{-1}. The H10-C5-H12 and H13-C7-H15 rocking modes calculated at 1080 cm^{-1} match well with the experimental band at 1090 cm^{-1}, indicating that the theoretical model accurately predicts these molecular deformations.

•High-Frequency Region (1300 – 1700 cm^{-1}):
The scissoring modes involving C-H and N-H bonds demonstrate good agreement, with the calculated peak at 1447 cm^{-1} corresponding to the experimentally observed peak at 1445 cm^{-1}. The asymmetric stretching mode of C8=N3 appears at 1564 cm^{-1} (calculated) and 1568 cm^{-1} (measured), reflecting the precision of the computational method in predicting bond.

Surface-Enhanced Raman Spectroscopy DFT Simulations of Metformin

SERS-DFT calculations provides valuable insights into molecular interactions at metal surfaces. In this study, DFT simulations were performed using a 10-gold atom cluster to model the adsorption of the target molecule, employing the LANL2DZ basis set for accurate representation of relativistic effects and electron correlation in gold. Before simulating the SERS spectrum, we modeled three different geometries of 10-gold atom cluster interacting with MET and selected the most energetically stable configuration for further calculations.

Figure 5 presents the optimized geometries of gold clusters (10 atoms) interacting with MET, where (a) and (c) depict different adsorption configurations, and (b) corresponds to the most stable structure based on energy calculations. In (a) and (c), MET interacts with the gold cluster in varying orientations, leading to differences in binding sites and spatial arrangements. In contrast, (b) adopts a more favorable configuration, maximizing interactions with the Au atoms while maintaining a stable adsorption geometry. The lower energy of (b) indicates stronger and more stable interactions, particularly due to the orientation of the terminal amine groups, which in this configuration establish stronger interactions with the gold surface, enhancing electronic coupling and stabilizing the adsorption. The MEP analysis of the gold cluster-MET complex provides insights into the charge distribution (Figure 5d), crucial for understanding its interaction with metal surfaces in SERS applications. The optimized configuration shows a strong charge localization in specific regions, suggesting potential hotspots for Raman enhancement. This configuration ensures a more reliable adsorption of MET on the Au surface, leading to accurate predictions of vibrational shifts and enhanced charge transfer interactions crucial for the SERS enhancement mechanism. Therefore, structure (b) was selected for the final SERS-DFT calculations to obtain a representative and reliable theoretical prediction of the experimental results.

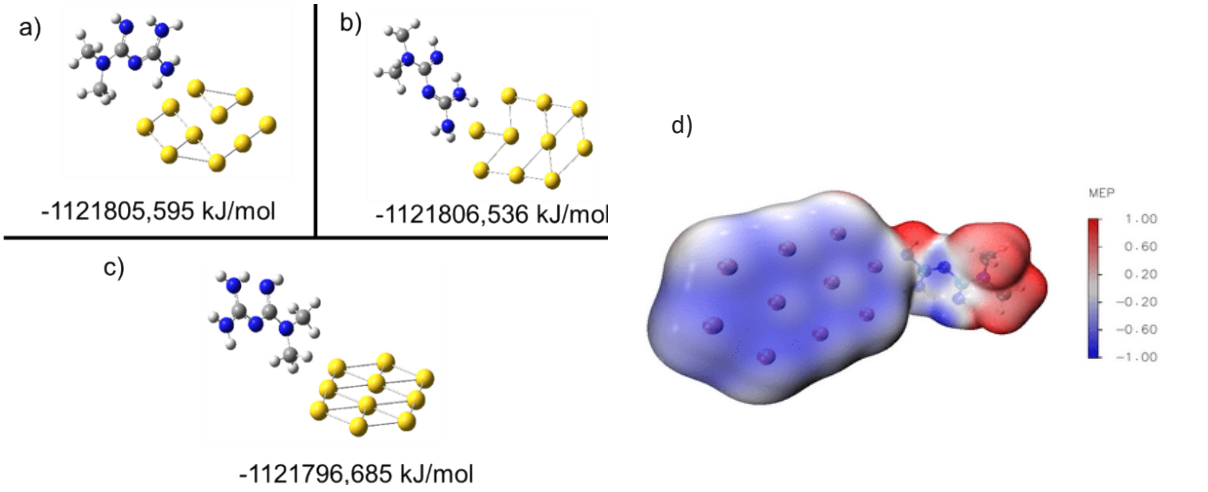

Figure 5. Optimized structures of 10-gold atom cluster interacting with metformin and Molecular electrostatic potential map of the gold cluster-MET complex. (a) First adsorption configuration; (b) Most stable adsorption configuration; (c) Third adsorption configuration and (d) MEP metformin-Au cluster.

The simulated SERS spectrum presented in Figure 5 (blue bottom) exhibits significantly higher intensity compared to the Raman spectrum (pink top), indicating strong enhancement due to the interaction of MET with the plasmonic surface (likely gold nanoparticles in the SERS substrate,

as seen in the molecular representation). This intensity increase suggests strong adsorption of MET onto the metallic nanostructure, which enhances Raman signals via electromagnetic and/or chemical enhancement mechanisms. Some Raman peaks shift slightly in the SERS spectrum, likely due to interactions between MET and the metal surface. These shifts indicate changes in molecular orientation or charge transfer effects. Certain vibrational modes are more pronounced in SERS than in Raman, which suggests selective enhancement of specific functional groups interacting with the substrate. The observed enhancement and shift of vibrational bands in the SERS spectrum of MET are primarily attributed to two factors: changes in molecular orientation on the metallic surface and charge transfer interactions between MET and the gold cluster. Upon adsorption, the terminal amine and guanidine groups of MET, which are rich in electron density as shown in the MEP map (Figure 3), interact directly with the Au atoms (Figure 5b), leading to chemisorption and redistribution of electronic charge. This interaction modifies the local polarizability of the molecule, selectively enhancing modes involving those functional groups. For example, the vibrational modes at 1009 and 1257 cm^{-1}, which involve C-H and N-H scissoring and rocking of groups near the gold surface, are significantly more intense in the SERS spectrum, indicating their direct involvement in surface interaction.

Furthermore, the shift in peaks such as the N-H rocking (from 430 to 426 cm^{-1}) and the C=N stretching mode (from 1564 to 1568 cm^{-1}) suggests that the adsorption alters bond strengths through charge delocalization. The molecular electrostatic potential (MEP) of the MET-Au complex (Figure 5d) reveals a redistribution of charge density compared to the free molecule, with localized negative potential near the Au-bound sites. This supports the presence of charge transfer from the metal to the molecule (or vice versa), consistent with the chemical enhancement mechanism in SERS. The molecule adopts a slightly tilted orientation over the gold cluster, aligning electron-donating groups toward the surface, which amplifies certain vibrational modes while suppressing others.

Thus, the selective enhancement observed in the SERS spectrum is not uniform but depends on both the proximity of functional groups to the metallic surface and the changes in electronic environment upon complex formation. These findings align with established theories on electromagnetic and chemical contributions to the SERS effect [1,2]. In both spectra, strong peaks appear in the range of 600 – 1600 cm^{-1}, corresponding to key vibrational modes of MET. The SERS spectrum shows enhanced peaks around 600 – 1000 cm^{-1}, which could be related to ring deformation, C-N stretching, and NH bending modes. Peaks above 1200 cm^{-1} correspond to C-H and N-H stretching, with some intensity variations due to surface interactions. The increased intensity of peaks related to C=N and NH bending (1300 – 1600 cm^{-1}) suggests that metformin's guanidine group plays a crucial role in adsorption suggesting that probably MET is effectively adsorbed onto the gold nanostructure. The enhanced SERS signal at 1009 cm^{-1} (H10-C5-H12, H13-C7-H15 scissoring) aligns with the Raman signal for MET. This signal could be useful for detecting MET in biological samples as blood plasma, serum, and urine [31]. Raman spectroscopy with this peak offers a non-invasive method for MET monitoring. Recent studies have demonstrated the usefulness of SERS for MET detection. Li *et al.* [43] combined solvent microextraction with SERS to detect metformin in spiked health products, achieving high sensitivity using Ag colloids. Hennemann *et al.* [44] studied the plasmonic interaction of MET with gold nanoparticles and reported SERS enhancement based on agglomeration and aggregation regimes. Unlike these experimental works, our study provides a theoretical perspective, offering DFT-based Raman and SERS simulations along with electrostatic potential analysis to understand the spectral behavior and adsorption mechanism of MET at the molecular level.

Conclusions

In conclusion, the computational analysis of MET through DFT simulations revealed crucial insights into its molecular geometry, electronic properties, and vibrational characteristics. The optimized geometry showed MET adopting a near-planar structure, with significant intramolecular hydrogen bonding, especially in the most stable conformer. Conformers b and c exhibited higher energy due to steric hindrance and repulsion between functional groups, highlighting the importance of molecular flexibility. The bond lengths and dihedral angles obtained were in good agreement with experimental data, with slight variations attributed to computational conditions. The molecular

electrostatic potential map demonstrated regions of high and low electron density, essential for understanding MET's interactions with metal surfaces in SERS. DFT-based Raman simulations revealed a strong correlation between calculated and experimental vibrational frequencies, with prominent peaks in the low, mid, and high-frequency regions, further supporting the theoretical model. The SERS-DFT simulations indicated that MET interacts strongly with gold nanoparticle surfaces, enhancing its Raman signals and providing a reliable method for detecting MET in biological samples. These findings underscore the potential of computational techniques in predicting molecular behavior and enhancing the application of Raman spectroscopy for MET monitoring in various settings.

Acknowledgements

Castillo J. acknowledge financial support from Otto Mønsted Foundation (Denmark) and Vicerrectoría de Investigaciones de la Universidad Industrial de Santander.

References

[1] Sui X, Xu Y, Wang X, Han W, Pan H, Xiao M. Metformin: A Novel but Controversial Drug in Cancer Prevention and Treatment. Mol Pharm. 2015;12(11):3783–91. https://doi.org/10.1021/acs.molpharmaceut.5b00577

[2] Mundaca-Uribe R, Holay M, Abbas A, Askarinam N, Sage-Sepulveda JS, Kubiatowicz L, *et al.* A Microstirring Oral Pill for Improving the Glucose-Lowering Effect of Metformin | ACS Nano. 2023;17(10):9272-79. https://doi.org/10.1021/acsnano.3c00581

[3] Tian JL, Si X, Shu C, Wang YH, Tan H, Zang ZH, *et al*. Synergistic Effects of Combined Anthocyanin and Metformin Treatment for Hyperglycemia *In Vitro* and *In Vivo*. J Agric Food Chem. 2022;70(4):1182–95. https://doi.org/10.1021/acs.jafc.1c07799

[4] Ala M, Ala M. Metformin for Cardiovascular Protection, Inflammatory Bowel Disease, Osteoporosis, Periodontitis, Polycystic Ovarian Syndrome, Neurodegeneration, Cancer, Inflammation and Senescence: What Is Next? ACS Pharmacol. Transl. Sci. 2021;4(6):1747-1770. https://doi.org/10.1021/acsptsci.1c00167

[5] He Y, Zhang Y, Ju F. Metformin Contamination in Global Waters: Biotic and Abiotic Transformation, Byproduct Generation and Toxicity, and Evaluation as a Pharmaceutical Indicator. Environ Sci Technol. 2022;56(19):13528–45. https://doi.org/10.1021/acs.est.2c02495

[6] Castillo JJ, Rindzevicius T, Rozo CE, Thamdrup LHE, Boisen A. Surface-enhanced Raman spectroscopy coupled with DFT for sensitive detection of tadalafil in complex matrices. Vib. Spectrosc. 2025;140:103847. https://doi.org/10.1016/j.vibspec.2025.103847

[7] Chao J, Wenfang C, Shao S, Lixing W, Shiping S, Chunhai F, *et al.* Nanostructure-based surface-enhanced Raman scattering biosensors for nucleic acids and proteins. J. Mater. Chem. B. 2016;4(10):1757-1769. https://doi.org/10.1039/C5TB02135A

[8] Jones CW. Nicholas Turner Selected To Deliver the Seventh *ACS Catalysis* Lectureship. ACS Catal. 2018;8(2):1601. https://doi.org/10.1021/acscatal.8b00261

[9] Rindzevicius T, Barten J, Vorobiev M, Schmidt MS, Castillo JJ, Boisen A. Detection of surface-linked polychlorinated biphenyls using surface-enhanced Raman scattering spectroscopy. Vib. Spectrosc. 2017;90:1–6. https://doi.org/10.1016/j.vibspec.2017.02.004

[10]Horne J. Pierre B, Pierre-Yves S, Charlotte DB, Pierre F, Nicolas T, *et al.* Optimisation of a Microwave Synthesis of Silver Nanoparticles by a Quality by Design Approach to Improve SERS Analytical Performances. Molecules. 2024;29(14):3442. https://doi.org/10.3390/molecules29143442

[11]Mandial D, Khullar P, Kumar H, Ahluwalia GK, Bakshi MS. Naringin–Chalcone Bioflavonoid-Protected Nanocolloids: Mode of Flavonoid Adsorption, a Determinant for Protein Extraction. ACS Omega. 2018;3(11):15606-614. https://doi.org/10.1021/acsomega.8b01776

[12]Karimi S, Tavassoli SH. The feasibility of Raman spectroscopy for accurate assessment of essential criteria in pharmaceutical industry by investigation of Metformin hydrochloride tableting process. J. Raman Spectrosc. 2024;55(6):688-694. https://doi.org/10.1002/jrs.6666

[13]Minh DTC, Thi LA, Huyen NTT, Van Vu L, Anh NTK, Ha PTT. Detection of sildenafil adulterated in herbal products using thin layer chromatography combined with surface enhanced Raman spectroscopy: "Double coffee-ring effect" based enhancement. J. Pharm. Biomed. Anal. 2019;174:340–7. https://doi.org/10.1016/j.jpba.2019.05.043

[14]Paul, SPM, Praveena G, Beula RJ, Haris M, Abiram A.Theoretical investigation on the interaction between Metformin and Ferulic acid - A DFT approach. J. Indian Chem. Soc. 2022;99(3):100368. https://doi.org/10.1016/j.jics.2022.100368

[15]Koglin E, Witte EG, Willbold S, Meier RJ. Evaluation of ab initio methods for the calculation of ^{13}C NMR shifts of metabolites of methabenzthiaruzon. J. Mol. Struct. (Theochem). 2004;712(1-2):233-237. https://doi.org/10.1016/j.theochem.2004.10.027

[16]Totsche KU, Rennert T, Gerzabek MH, Kögel-Knabner I, Smalla K, Spiteller M, *et al*. Biogeochemical interfaces in soil: The interdisciplinary challenge for soil science. JPNSS. 2010;173(1):88–99. https://doi.org/10.1002/jpln.200900105

[17]Islam MdA, Hossain N, Ahsan Z, Rana M, Rahman M, Abdullah Md. DFT insights into the mechanical properties of NMs. Results Surf. Interfaces. 2025;18:100417. https://doi.org/10.1016/j.rsurfi.2025.100417

[18]Borisov YA, Akhrem IS. DFT B3LYP/6-311+G* calculation study of a new nonclassical mechanism of electrophilic functionalization of aromatic C–H bond via aryl cation formation. Mendeleev Commun. 2019;29(3):343-345. https://doi.org/10.1016/j.mencom.2019.05.035

[19] Ganiev B, Mardonov U, Kholikova G. Molecular structure, HOMO-LUMO, MEP - – Analysis of triazine compounds using DFT (B3LYP) calculations. Mater. Today Proc. 2023. https://doi.org/10.1016/j.matpr.2023.09.191

[20]Zhou Z, Song J, Xie Y, Ma Y, Hu H, Li H, *et al.* DFT calculation for organic semiconductor-based gas sensors: Sensing mechanism, dynamic response and sensing materials. Chin. Chem. Lett. 2025;36(6):110906. https://doi.org/10.1016/j.cclet.2025.110906

[21]Kim S, Piao L, Han D, Kim BJ, Chung TD. Surface Enhanced Raman Scattering on Non-SERS Active Substrates and In Situ Electrochemical Study based on a Single Gold Microshell. Adv. Mater. 2013;25(14):2056–61. https://doi.org/10.1002/adma.201203187

[22]Karthick Kannan, P, Shankar P, Blackman C, Chung CH. Recent Advances in 2D Inorganic Nanomaterials for SERS Sensing. Adv. Mater. 2019;31(34):1803432. https://doi.org/10.1002/adma.201803432

[23]Dumont E, Castillo JJ, Rozo CE, Zappalá G, Slipets R, Thamdrup LHE, *et al.* Vibrational study of mycophenolic acid and its quantification with electrochemically assisted surface-enhanced Raman spectroscopy. Sens. Actuators B: Chem. 2024;417:136126. https://doi.org/10.1016/j.snb.2024.136126

[24]Castillo JJ, Rindzevicius T, Rozo CE, Boisen A. Adsorption and Vibrational Study of Folic Acid on Gold Nanopillar Structures Using Surface-Enhanced Raman Scattering Spectroscopy. Nanomaterials and Nanotechnology. 2015;5:29. https://doi.org/10.5772/61606

[25]Chen LM, Liu YN. Surface-Enhanced Raman Detection of Melamine on Silver-Nanoparticle-Decorated Silver/Carbon Nanospheres: Effect of Metal Ions. ACS Appl. Mater. Interfaces 2011;3(8):3091–3096. https://doi.org/10.1021/am200603y

[26]Vo-Dinh T, Wang HN, Scaffidi J. Plasmonic nanoprobes for SERS biosensing and bioimaging J. Biophotonics. 2010;3(1-2):89-102. https://doi.org/10.1002/jbio.200910015

[27]Rozo C, Wu K, Rindzevicius T, Boisen A, Castillo JJ. Surface-enhanced Raman Spectroscopy and Density Functional Theory Study of Glyphosate and Aminomethylphosphonic acid Using Silver Capped Silicon Nanopillars. Univ. Sci. 2021;26(1):51–66. https://doi.org/10.11144/Javeriana.SC26-1.srsa

[28]Cao YC, Jin R, Nam JM, Thaxton CS, Mirkin CA. Raman Dye-Labeled Nanoparticle Probes for Proteins. J. Am. Chem. Soc. 2003;125(48):14676–7. https://doi.org/10.1021/ja0366235

[29]Yang G, Nanda J, Wang B, Chen G, Hallinan DT. Self-Assembly of Large Gold Nanoparticles for Surface-Enhanced Raman Spectroscopy. ACS Appl. Mater. Interfaces. 2017;9(15):13457–70. https://doi.org/10.1021/acsami.7b01121

[30]Qu X, Qi G, Sun D, Yue J, Xu W, Xu S. Metformin hydrochloride action on cell membrane N-cadherin expression and cell nucleus revealed by SERS nanoprobes. Talanta. 2021;232:122442. https://doi.org/10.1016/j.talanta.2021.122442

[31]Castillo JJ, Rozo CE, Castillo-León J, Rindzevicius T, Svendsen WE, Rozlosnik N, *et al*. Computational and experimental studies of the interaction between single-walled carbon nanotubes and folic acid. Chem. Phys. Lett. 2013;564:60–64. https://doi.org/10.1016/j.cplett.2013.02.014

[32]Mackoy T, Kale B, Papka ME, Wheeler RA. viewSq, a Visual Molecular Dynamics (VMD) module for calculating, analyzing, and visualizing X-ray and neutron structure

factors from atomistic simulations. Comput. Phys. Commun. 2021;264:107881. https://doi.org/10.1016/j.cpc.2021.107881

[33]Janani S, Rajagopal H, Sakthivel S, Aayisha S, Raja M, Irfan A, *et al*. Molecular structure, electronic properties, ESP map (polar aprotic and polar protic solvents), and topology investigations on 1-(tert-Butoxycarbonyl)-3-piperidinecarboxylic acid-Anticancer therapeutic agent. J. Mol. Struct. 2022;1268:133696. https://doi.org/10.1016/j.molstruc.2022.133696

[34]Castillo JJ, Rozo CE, Bertel L, Rindzevicius T, Mendez-Sanchez SC, Ortega FM, *et al*. Orientation of pterin-6-carboxylic acid on gold capped silicon nanopillars platforms: Surface enhanced Raman spectroscopy and density functional theory studies. J. Braz. Chem. Soc. 2016;27(5):971–7. https://doi.org/10.5935/0103-5053.20150352

[35]Alsawat M, El-Sheshtawy HS, Altalhi T, Mezni A, Kumeria T, Al-Juaid SS, *et al*. Spectral and Structural Characterization of Metformin with Different Counter Anions: Comparative Analysis and DFT Calculations. Asian J. Chem. 2021;33(11):2817–25. https://doi.org/10.14233/ajchem.2021.23422

[36]Mondal S, Samajdar RN, Mukherjee S, Bhattacharyya AJ, Bagchi B. Unique Features of Metformin: A Combined Experimental, Theoretical, and Simulation Study of Its Structure, Dynamics, and Interaction Energetics with DNA Grooves. J. Phys. Chem. B. 2018;122(8):2227–2242. https://doi.org/10.1021/acs.jpcb.7b11928

[37]Wang B, Zhong Z, Hou Y, Zhao X, Zhang P, Wei J, *et al*. Biomanufacturing of food-grade citric acid and comprehensive utilization of its production wastewater. Food Sci. Technol. 2023;43:e110422. https://doi.org/10.1590/fst.110422

[38]Cai L, Jiang L, Li C, Guan X, Zhang L, Hu X. Multicomponent Crystal of Metformin and Barbital: Design, Crystal Structure Analysis and Characterization. Molecules. 2021;26(14):4377. https://doi.org/10.3390/molecules26144377

[39]Ghasemi F, Rezvani AR, Ghasemi K, Abdul Razak I, Rosli MM. Synthesis, characterization and crystal structure of a new organic salt of antidiabetic drug metformin resulting from a proton transfer reaction. J. Mol. Struct. 2019;1193:310–4. https://doi.org/10.1016/j.molstruc.2019.05.040

[40]Saeed A, Bosch A, Bettiol M, Nossa González DL, Erben MF, *et al*. Novel Guanidine Compound against Multidrug-Resistant Cystic Fibrosis-Associated Bacterial Species. Molecules. 2018;23(5):1158. https://doi.org/10.3390/molecules23051158

[41]Castillo JJ, Rindzevicius T, Wu K, Rozo CE, Schmidt MS, Boisen A. Silver-capped silicon nanopillar platforms for adsorption studies of folic acid using surface enhanced Raman spectroscopy and density functional theory. J. Raman Spectrosc. 2015;46(11):1087–94. https://doi.org/10.1002/jrs.4734

[42]Bayramov FB, Toporov VV, Chakchir OB, Anisimov VN, Rud VY, Glinushkin AP, *et al*. Raman spectroscopic characterization of anti-diabetic drug metformin hydrochloride J. Phys.: Conf. Ser. 2019;1400(3):033010. https://doi.org/10.1088/1742-6596/1400/3/033010

[43]Yang L, Sun Z, Zhang L, Cai Y, Peng Y, Cao T, *et al.* Chemical labeling for fine mapping of IgG N-glycosylation by ETD-MS. Chem Sci. 2019;10(40):9302–7. https://doi.org/10.1039/C9SC02491C

[44]Hennemann AL, Ramos MD, Sihn LM, Nakamura M, Araki K, Toma HE. Plasmonic Interaction of Gold Nanoparticles with the Anti-hypoglycemic Medicament Metformin. Plasmonics 2025;20:793–801. https://doi.org/10.1007/s11468-024-02341-1